OPEN ACCESS
IOP Publishing | Songshan Lake Materials Laboratory
Materials Futures
Mater. Futures 3 (2024) 035401 (11pp)
https://doi.org/10.1088/2752-5724/ad47ce

Biomimetic artificial islet model with vascularized microcapsule structures for durable glycemic control

Jingbo Li[1,2], Yile Fang[3,4], Zhuhao Wu[4], Luoran Shang[3,4,*] and Ling Li[1,2,*]

[1] Department of Endocrinology, Zhongda Hospital, School of Medicine, Southeast University, Nanjing 210009, People's Republic of China
[2] Institute of Glucose and Lipid Metabolism, Southeast University, Nanjing 210009, People's Republic of China
[3] Shanghai Xuhui Central Hospital, Zhongshan-Xuhui Hospital, and the Shanghai Key Laboratory of Medical Epigenetics, The International Co-laboratory of Medical Epigenetics and Metabolism (Ministry of Science and Technology), Institutes of Biomedical Sciences, Fudan University, Shanghai 200032, People's Republic of China
[4] Department of Clinical Laboratory, Nanjing Drum Tower Hospital, The Affiliated of Medical School, Nanjing University, Nanjing 210008, People's Republic of China

E-mail: luoranshang@fudan.edu.cn and lingli@seu.edu.cn

Received 26 February 2024, revised 24 April 2024
Accepted for publication 5 May 2024
Published 24 May 2024

Abstract

Islet transplantation is a promising strategy for diabetes mellitus treatment as it can recapitulate endogenous insulin secretion and provide long-term glycemic control. Islet models constructed in biomaterial scaffolds that reproduce biological characteristics of native islets is a feasible option to circumvent the dilemma of donor shortage and the requirement of chronic immunosuppression. Herein, we developed bioinspired artificial microcapsule-based islet models with microvessels for glycemic control using microfluidic electrospray strategy. Microfluidic electrospray can generate uniform hydrogel microcapsules with core-shell structure for encapsulating islet cells. The cell-laden microcapsules enabled the efficient transportation of nutrient, oxygen, and insulin; as well as the incorporation with microvessels for prompting glucose responsiveness and molecular exchange. We demonstrated by *in vivo* experiments that the blood glucose, food intake, and body weight of diabetic mouse models were alleviated, and the glucose tolerance was promoted after the engraftment of islet microcapsules. We further demonstrated the improved functionality of transplanted islet model in insulin secretion, immune escape, and microcirculation using standard histological and molecular analysis. These results indicated that the microcapsules with microvessels are promising artificial islet models and are valuable for treating diabetes.

Supplementary material for this article is available online

Keywords: artificial islet model, microfluidics, vascularization, hydrogel, diabetes

* Authors to whom any correspondence should be addressed.

1. Introduction

Diabetes mellitus (DM) is a common metabolic disease manifested by islet injury [1]. Therapeutic efforts have been made to treat diabetes such as insulin injection. Although exogenous insulin supply alleviates blood glucose levels temporally, the need for frequent injections causes huge burdens and severe adverse complications may occur [2–4]. As an alternative strategy that recapitulates endogenous insulin secretion, islet transplantation is promising for long-term glycemic control [5, 6]. However, the donor shortage and the required chronic immunosuppression in the islet transplantation pose great challenges in the DM therapeutics [7]. In view of this, biomaterial scaffolds encapsulating islet or islet cells have been developed to reconstruct islet functions, such as restoring glucose homeostasis [8–10]. Although rapid progress has been achieved, biomaterial-based islet models with long-term survival and sustained insulin secretion functions are impeded by immune attack as well as insufficient nutrient and oxygen supply [7]. Therefore, novel artificial islet models that reproduce biological characteristics of native islets is still anticipated for improving their functionality in achieving more effective and sustained glycemic control.

In this paper, inspired by the intrinsic architecture of human islets, we designed a type of biomimetic 'artificial islet' with vascularized microcapsule structures by using microfluidic electrospray technology (figure 1). Leveraging its precise fluidic manipulation capabilities, microfluidics has been widely utilized in the production of hydrogel microparticles with customizable structures including porous [11–13], core-shell [14–19], and multi-compartmental [20–22], etc. [23–30]. The incorporation of islet cells in these microgels takes advantage of their large surface area, facilitating efficient oxygen and nutrient exchange [31–33]. Furthermore, the adaptable structural characteristics of microgels enable the co-encapsulation of additional agents capable of further regulating cell fate [34–38]. Despite these merits, accurately reproducing the complete structure of native islets remains challenging. Shortcomings such as inadequate vascularization limit the functional capabilities of existing microgel scaffolds [39, 40].

Herein, we constructed a unique artificial microphysiological islet model by coculturing islet and endothelial cells for establishing a vascularized islet model. Core-shell microcapsules were generated via microfluidic electrospray, which were loaded with pancreatic β cells and microvessels derived from human umbilical vein cells (HUVECs). Taking advantages of the hydrogel shield, β cells can be physically isolated from host immune cells and thus escaping from immune attack. Moreover, the presence of microvessels improved the exchange of biological substances. Together, the microcapsules could facilitate nutrient, oxygen, and insulin delivery. Based on this, the microcapsules were transplanted to diabetic mice to achieve sustained control of elevated blood glucose levels. It was found that the transplanted grafts effectively mitigated conditions including hyperglycemia, weight loss, and polyphagia. These results indicated the value of this artificial islet model in durable glycemic control, and potential applications are expected in diabetes treatment, tissue engineering, and regenerative medicine.

2. Experimental sections

2.1. Materials

Sodium alginate (ALG), carboxymethyl cellulose sodium (CMC), and calcium chloride ($CaCl_2$) were obtained from Aladdin. Cell counting kit-8 (CCK8) and the Calcein AM (CAM)/PI staining kit was purchased from Beyotime, China. Anti-Insulin antibody, bovine fibrinogen and thrombin were obtained from Sigma. FITC-Dextran at 4 kDa, 70 kDa, and 150 kDa were obtained from Xi'an ruixi Biological Technology Co., Ltd Krebs Ringer Buffer (KRB) was purchased from Solarbio. Insulin-producing β cells line (MIN6) purchased from American type culture collection were cultured in DMEM containing 10% FBS (Merck), supplemented with 1% penicillin-streptomycin solution (Gibco), and 50 μM β-mercaptoethanol (Gibco) at 37 °C in an incubator with 5% CO_2. Medium was replaced every other day. HUVECs were cultured in EGM-2 (Lonza), which is supplemented with the optimized growth factors and 2% FBS.

2.2. Microfluidic device construction

The microfluidic electrospray device was mainly composed of two glass capillaries assembled on a glass slide. The two capillaries were tapered to reach diameters of 100 μm and 500 μm respectively, serving as the inner and outer tubes. Subsequently, the outer tube, nesting the inner tube coaxially, was affixed onto the glass slide with transparent epoxy resin. Finally, the connections were sealed with needles for pumping liquids into each tube.

2.3. Fabrication of vascularized artificial islet microcapsules

The artificial islet microcapsules were generated by the microfluidic electrospray system. The inner phase consisted of a mixture of 1 wt% CMC and MIN6 at the concentration of 5×10^4 cells ml^{-1}. The outer phase comprised 1 wt% ALG. The respective liquids were accurately pumped into the corresponding tubes by micropumps (LSP-01-2A, Longer-Pump, China) via polyethylene tubes. At the outlet of the microfluidic device, monodispersed droplets were fabricated under an electric field (provided by Dongwen high voltage power supply (Tianjin) Co., Ltd). Subsequently, the microdroplets were collected in 2 wt% $CaCl_2$ for crosslinking of ALG. The flow rates of the outer and inner phases could be controlled by the syringe pumps, while the voltage and distance between the microfluidic device outlet and the ground could also be adjusted for optimal droplet formation. For *in vitro* and *in vivo* experiments encapsulating cells, parameters of the microfluidic system were set as: 1 wt% CMC, 1 wt% ALG, $F_{\text{outer}} = 80$ μl min^{-1}, $F_{\text{inner}} = 20$ μl min^{-1}, $U = 5$ kV, $d = 2$ cm.

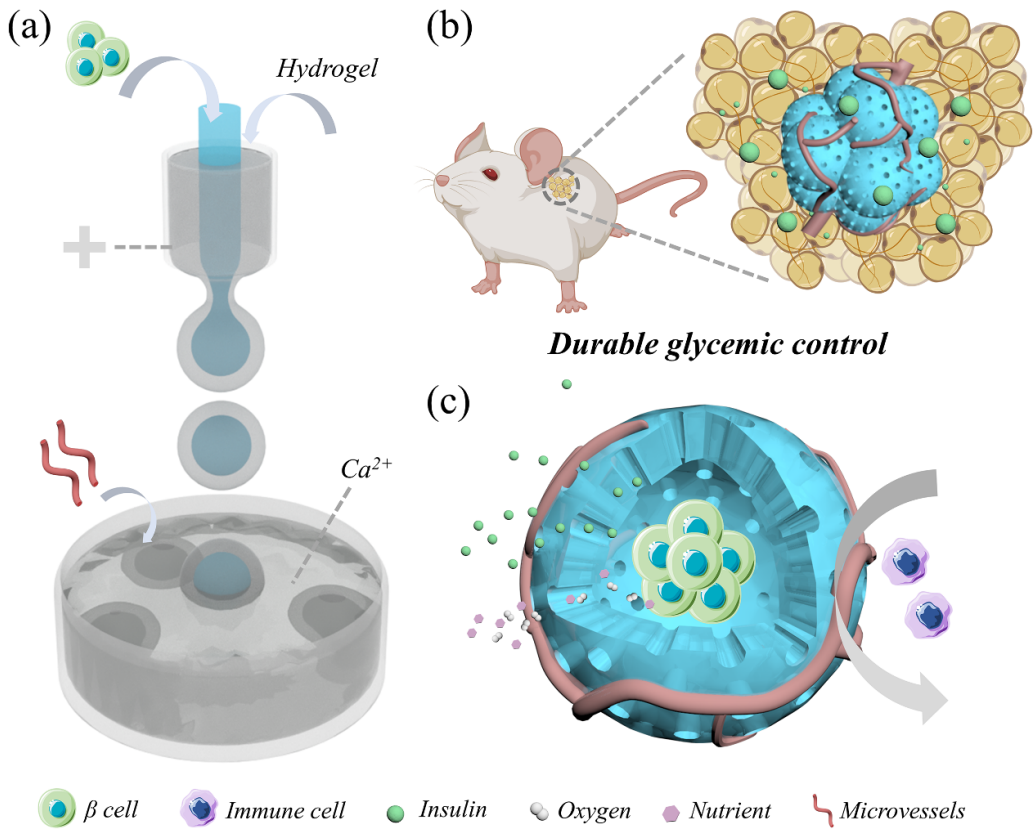

Figure 1. Schematics of biomimetic artificial islet model with vascularized microcapsule structures for durable glycemic control. (a) Fabrication of microcapsules by using microfluidic electrospray strategy. (b) Transplantation of vascularized microcapsules on the dorsal brown adipose tissue of diabetic mouse. The transplanted microcapsules secrete insulin for relieving hyperglycemia. (c) The microcapsules allow for the perfusion of nutrient and oxygen, and the release of insulin from pancreatic β cells, while hindering the attack of host immune cells.

To construct a vascular network for the artificial islet, HUVECs were co-cultured with the as-prepared islet microcapsules in a 5 mg ml^{-1} bovine fibrinogen solution. HUVECs and normal human lung fibroblasts (NHLFs) were digested and dispersed in the medium. Then, the fibrinogen solution was prepared containing 3×10^6 cells ml^{-1} HUVECs, 5×10^6 cells ml^{-1} NHLFs, and ≈3000 microcapsules ml^{-1}. After mixing 5 U ml^{-1} thrombin, the mixture was placed in the incubator for 30 min. The cell-laden composite gel constructs were then submerged with the formulated medium (RPMI-1640: Endothelial Growth Medium, EGM-2, 1: 1). For maintaining cell culture, the medium was replaced every other day. The vascular networks could be observed around the 3rd day of incubation.

2.4. Characterization

The microcapsules were observed by an optic microscope equipped with a CCD camera (OLYMPUS IX71, and DP30BW). Scanning electron microscopic (SEM) (HITACHI, S3000N) was used to investigate the microstructures of the microcapsules. To observe the vascular structures, F-actin and DAPI were used to label the cytoplasm and nucleus of HUVECs and NHLFs, respectively.

Insulin-FITC (1 mg ml^{-1}) and Rhodamine B (1 mg ml^{-1}) were used to evaluate the molecular permeation capacity of the microcapsules. The fabricated microcapsules were emersed in the Rhodamine B solution to simulate the entrance of small molecules. To simulate the release of insulin from the cells, the Insulin-FITC solution was used as the inner phase of the microfluidic system, which was then encapsulated in the microcapsules. The parameters of microfluidic system were consistent with those employed in other *in vitro* and *in vivo* experiments, as mentioned before. In specific time points, images were taken with a fluorescent microscope (Carl Zeiss, Germany). To evaluate the immunoprotecting capacity, 1 mg ml^{-1} FITC-Dextran at 4 kDa, 70 kDa, and 150 kDa were encapsulated in the microcapsules, respectively. At specific time points, microcapsules were evaluated using immunofluorescent microscopy (Carl Zeiss, Germany). Image analysis was conducted using Image J software to determine the maximum fluorescence intensity of FITC-Dextran inside the microcapsule, as well as the fluorescence intensity of the solution outside the microcapsule. Subsequently, a ratio of internal to external fluorescence was calculated, with a ratio of 1 indicating identical fluorescence intensity between the microcapsule and the surrounding solution. The results are presented as the ratio of internal to external fluorescence over time.

2.5. In vitro *biocompatibility*

The viability of MIN6 cells was evaluated by CAM/PI staining and CCK8 assays. CAM/PI staining was employed for the detection of live/dead cells. CCK8 assays were conducted at 24 h, 48 h and 72 h of culture to perform quantitative assessment of cell viability. The testing samples were exposed to 10 μl/well of CCK8 PBS solution for 2 h at 37 °C. A microplate reader (SYNERGY HTX) measured the optical density of the samples at 450 nm.

2.6. *Insulin secretion detection*

To measure insulin secretion, MIN6 cells were starved in KRB with 2 mM glucose for 1 h. Afterwards, the cells were treated with fresh KRB containing 2 mM and 25 mM glucose for 1 h incubation each to measure insulin secretion at the low and high glucose level, respectively. The supernatants were then collected for secreted insulin detection. The glucose-stimulated insulin secretion (GSIS) indexes were estimated by dividing the insulin concentration secreted at 25 mM glucose by that at 2 mM glucose. All insulin levels were measured by using ultrasensitive mouse insulin ELISA kit (Beyotime, China).

2.7. In vivo *transplantation*

Male C57BL/6 mice, aged 8–10 weeks, were purchased from Shanghai Sipo-Bikai laboratory animal Company Limited. All animals were handled in strict accordance with the Guide for the Care and Use of Laboratory Animals of the National Institutes of Health, USA. The experimental protocols and animal care procedures were supervised and approved by Animal Investigation Ethics Committee of Southeast University (No. 20220304007).

Mice were peritoneally administrated with 150 mg kg^{-1} streptozotocin to establish the diabetic model after overnight fasting. The successful establishment of diabetic mice was confirmed by the blood glucose concentration exceeding 16.7 mmol l^{-1} in two independent tests on different days. Then, the successfully established mice models were allocated into four groups and received respective graft transplantsinto their dorsal adipose tissues. MCs or v-MCs were prepared 5 d prior to transplantation. For the v-MCs and MCs groups, the diabetic mice were transplanted with artificial islet microcapsules with or without microvessels, respectively. As for the Cells group, the diabetic mice were transplanted with naked MIN6 cells; while in the DM group, the diabetic mice underwent sham surgery and treated with normal saline. Non-fasting blood glucose levels were observed every 3 d post transplantation. Additionally, food intake and body weight were synchronously monitored with the blood glucose levels. At 28 d post transplantation, intraperitoneal glucose tolerance test (IPGTT) was conducted for evaluating glucose tolerance. Diabetic mice underwent fasting for 16 h before injecting glucose intraperitoneally. For recording the fluctuations of blood glucose under stimuli, the blood samples of mice were obtained for glucose evaluation at 0, 15, 30, 60, 90, and 120 min. At 42 d post transplantation, grafts were removed from the transplant site. At 14 d post graft removal, the visceral organs of sacrificed mice such as pancreas, liver, heart, kidney, lung, and spleen were collected and fixed for histological analyses. Immunohistochemical staining and hematoxylin and eosin (HE) were conducted according to protocols. Tissue slices were observed under optical microscopy.

2.8. *Statistical analysis*

All statistical analyses were conducted with SPSS 20.0. The data were presented as mean ± standard deviation. Statistical significance of the difference was determined by students' *t*-test, one way ANOVA, and Kaplan–Meier analysis. $P < 0.05$ was considered significant.

3. Results and discussion

3.1. *Development of vascularized microcapsules as artificial islet models*

In a typical experiment, microcapsules were fabricated via microfluidic electrospray (figure 2(a)). A microfluidic device was constructed, consisting of two coaxially-nested glass capillaries, one as the inner tube and the other as the outer tube [41, 42]. A ALG solution flowed through the outer phase tube and a CMC solution with pancreatic islet β cells MIN6 flowed through the inner tube. Two-phase fluids were subjected to electrospray and formed uniform core-shell droplets at the outlet of microfluidic device (figure 2(c)). The electrostatic apparatus offered a high voltage, providing shear forces for controlling droplet sizes. Droplets were then collected in a calcium chloride solution, where they acquired a hydrogel shell due to the rapid crosslinking between ALG and Ca^{2+}. By controlling the conditions of the electrostatically driven microfluidic system, including the voltage, the distance between the orifice and the collecting pool, and the inner and outer flow rate, the diameter of the microcapsules could be tailored within a certain range (figure S1). Additionally, the microcapsules exhibited good monodispersity in size under all tested conditions (figure S2). Thus, size-uniform hydrogel microcapsules can be robustly generated, suggesting a potential application in cell encapsulations.

The as-prepared microcapsules were characterized under an optical microscope, which displayed a uniform spherical shape with a transparent shell (figures 2(b) and (e)). In addition, the cross-section SEM images demonstrated the core-shell architecture of the microcapsules (figures 2(d) and (f)). It was shown that cells were encapsulated inside the microcapsule. The hydrogel shell provides a physical shield to protect cells encapsulated in the core from immune attack. Mirroring the role of natural islets in insulin secretion, we tested this function by examining the permeation of model molecules through the microcapsules. It was found that insulin-FITC and small molecule Rhodamine B permeated through the microcapsule efficiently (figure S3). Based on this, we reasoned that

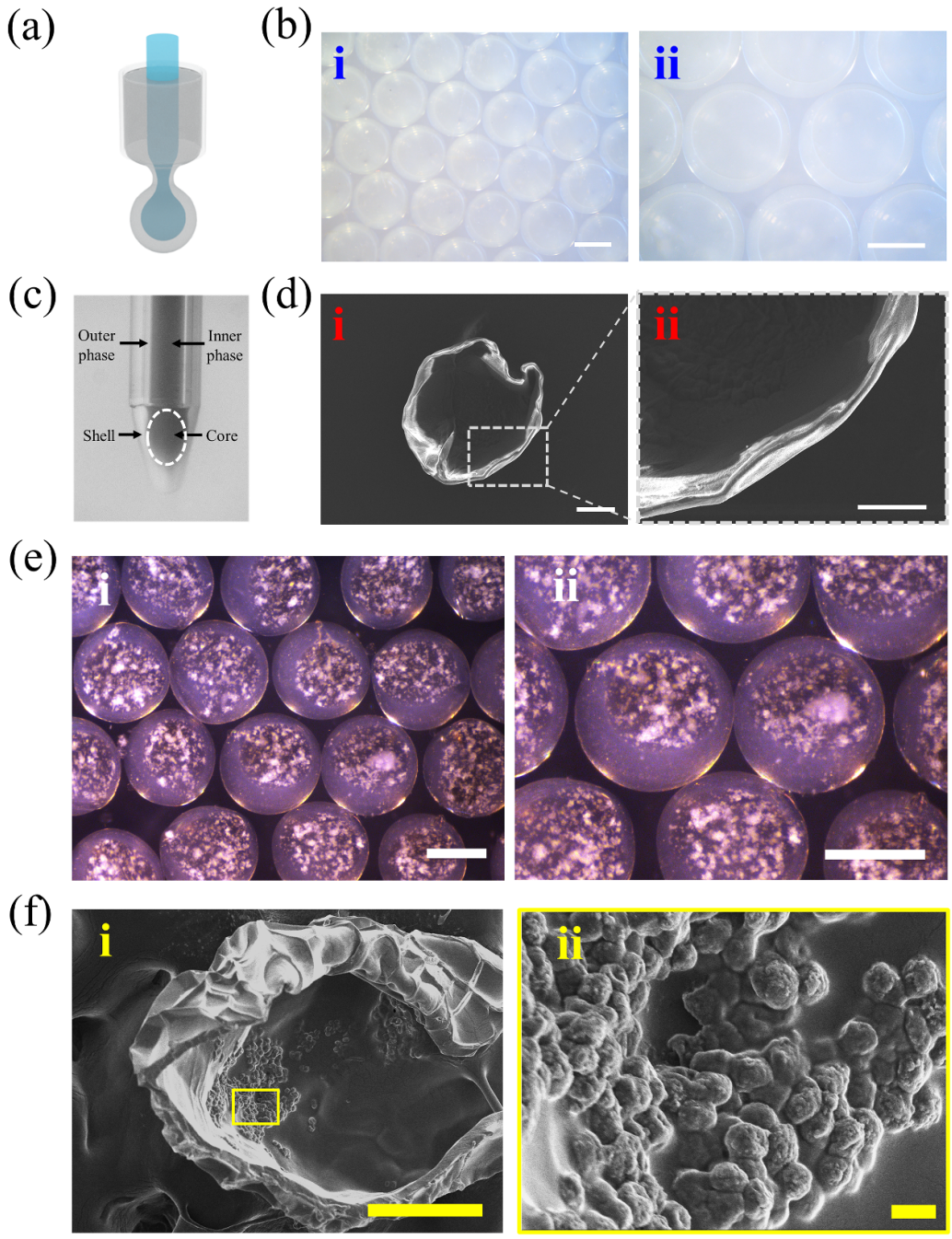

Figure 2. Fabrication and characterization of the microcapsules based on microfluidic electrospray. (a) Schematic of the microfluidic electrospray system. (b) Bright field microscopic images of the microcapsules at (i) low and (ii) high magnifications. Scale bar is 500 μm. (c) The real-time image of the microfluidic electrospray process. (d) SEM images of a dissected microcapsule at (i) low and (ii) high magnifications. Scale bar is 200 μm in (i) and 50 μm in (ii). (e) Microcapsules loading with MIN6 cells at (i) low and (ii) high magnifications. Scale bar is 500 μm. (f) SEM images of a dissected microcapsule loading with MIN6 cells at (i) low and (ii) high magnifications. Scale bar is 200 μm in (i) and 10 μm in (ii).

the microcapsules would allow for transferring nutrient and oxygen, as well as release of insulin. To evaluate the immunoprotecting capacity, FITC-Dextran at different molecular weight were used for determining the molecular weight cut-off of the microcapsule. Since the small molecular effectors of the host's immune system vary from 150 kDa to 900 kDa, FITC-Dextran at 4 kDa, 70 kDa, and 150 kDa were encapsulated in the microcapsule for the assays. It was demonstrated that FITC-Dextran at 4 kDa and 70 kDa permeated through the microcapsule, while the 150 kDa failed to enter the hydrogel (figure S4). These results suggested that the microcapsule fabricated selectively passes nutrients, glucose, as well as insulin, while protecting cells from the host's immune system.

To establish a vascular structure, HUVECs and NHLFs were co-cultured in a matrix composed of fibrinogen. After 3 d of cultivation, abundant microvessels and vascular

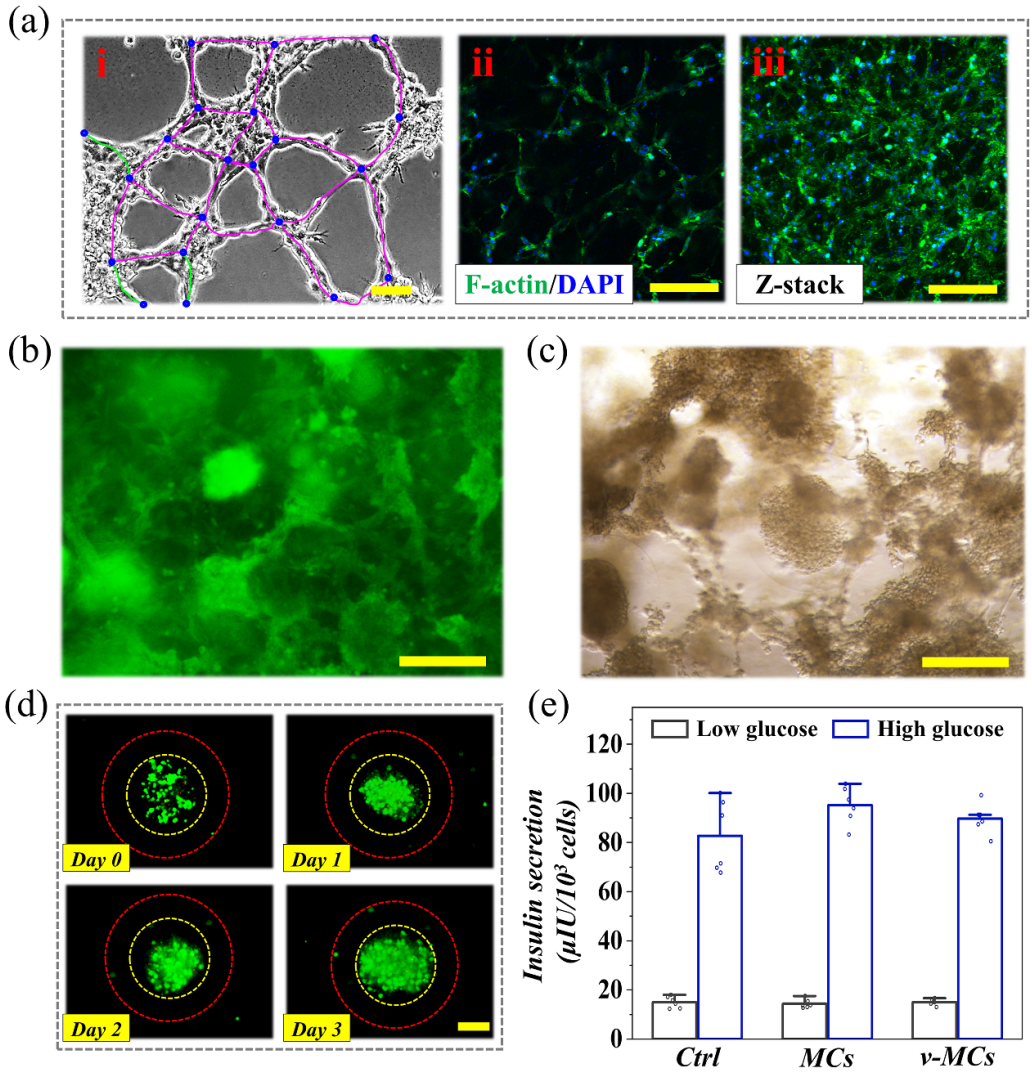

Figure 3. Cell proliferation and insulin secreting function of the vascularized microcapsules. (a) HUVECs formed vasculatures in the fibrinogen matrix at day 3. (i) Vasculatures were shown in closed purple loops; blue dots indicated the branch nodes; green lines demonstrate the branches extended by cells. (ii), (iii) HUVECs and NHLFs were stained green by F-actin at top view (ii) and side view (iii). Scale bar is 200 μm in (i), and 100 μm in (ii), (iii). (b) The microcapsules with the microvessels. Cells were stained with green by Calcein AM. Scale bar is 500 μm. (c) The bright field image of the microcapsules with the microvessels. Scale bar is 500 μm. (d) Representative microscopic and Calcein AM/PI staining images of the microcapsules at day 0, 1, 2 and 3. Yellow dotted circles represent the core of the microcapsules with islet cells encapsulated. Red dotted circles represent the hydrogel shell of the microcapsules. Live cells were stained green. Dead cells were stained red. Scale bar is 200 μm. (e) Measured insulin secretion of islet cells in planar dish cultivation or encapsulated in microcapsules with or without microvessels by GSIS assays. Ctrl: the control group; MCs: the artificial islet microcapsule group; v-MCs: the vascularized artificial islet microcapsule group.

network were formed. Microvessels were stained green by F-actin labeling and observed under confocal microscopy (figure 3(a)). To further construct vascularized microcapsules, MIN6 cells were co-cultured with HUVECs and NHLFs. It was found that the cells spread over the microcapsules at day 3 (figures 3(b) and (c)), indicating the intense vascularized structure of the microcapsules.

3.2. In vitro *viability and insulin secretion function*

To confirm the cell compatibility of the artificial islet, we assessed cell viability and proliferation under various culture conditions. For evaluating the survival of islet cells cultured in the microcapsules, fluorescent images were taken during the culture at day 0, 1, 2, and 3 (figure 3(d)). The CAM/PI staining was used to label live/dead cells with green/red, and the results indicated cell survival within the microcapsules for 7 d. For quantification of the cell viability, CCK8 assays were performed at 24 h, 48 h, and 72 h. It was found that the cell proliferation in microcapsules without microvessels (MCs) was comparable to that of planar dish culture (the control group, Ctrl). Moreover, the microcapsules with microvessels (v-MCs) showed comparable viability with the control group, as well as the MCs group (figure S5). These results indicated that the

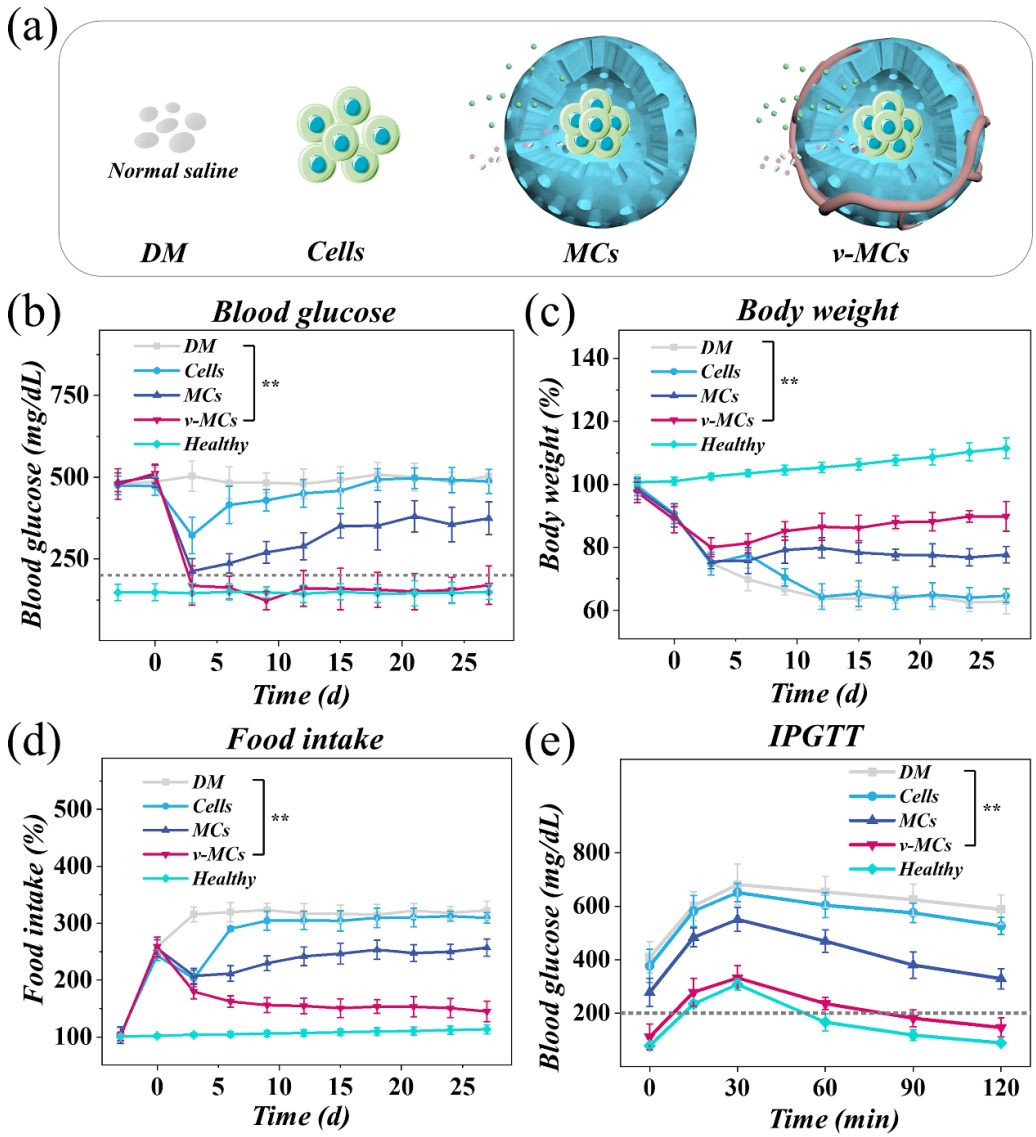

Figure 4. Transplantation of the vascularized artificial islet microcapsules and their *in vivo* therapeutic performances. (a) Schematic of the experimental groups. (b)–(d) Continuous monitoring of (b) blood glucose level, (c) body weight, and (d) food intake in different groups ($n = 5$). (e) Glucose responsiveness of diabetic mice receiving IPGTT at 28th day post transplantation ($n = 5$). The dotted line in (b) and (e) represents 200 mg dl^{-1}, which is the threshold of blood glucose level for diagnosing diabetes. Statistical analyses were conducted by using Kaplan–Meier analysis. $^{**}p < 0.01$. Healthy: the healthy control group; DM: the diabetes group; MCs: the artificial islet microcapsule group; v-MCs: the vascularized artificial islet microcapsule group.

fabricated artificial islet had good biocompatibility, and the encapsulated cells maintained good survival.

As pancreatic islet β cells hold the capacity of insulin secretion under stimuli, the GSIS assays were performed to evaluate the glucose responsiveness of the artificial islet. The insulin-secreting MIN6 cells in the Ctrl, MCs, and v-MCs groups were sequentially subjected to low and high glucose solutions. Although no significant differences were found in the GSIS assays, it was noted that the amount of insulin secreted from v-MCs increased by 6.35 folds under stimuli compared with basal level of insulin secretion, which was higher than that of control (5.52 folds) and MCs (5.98 folds) groups (figure 3(e)). This might be resulted from the 3D culture microenvironment of the microcapsules, which facilitates intracellular interactions and thus prompts their function of insulin secretion.

3.3. In vivo *transplantion and blood glucose control*

To further evaluate the *in vivo* function in blood glucose control, vascularized artificial islet microcapsules were conducted in a diabetic mouse model (figures 4(a) and S6). Mice with diabetes were transplanted with the constructed v-MCs at dorsal brown adipose tissues, as indicated by the *in vivo* imaging system (figure S7). The brown adipose tissues have a highly vascularized and anti-inflammatory microenvironment, which can promote graft survival while delaying

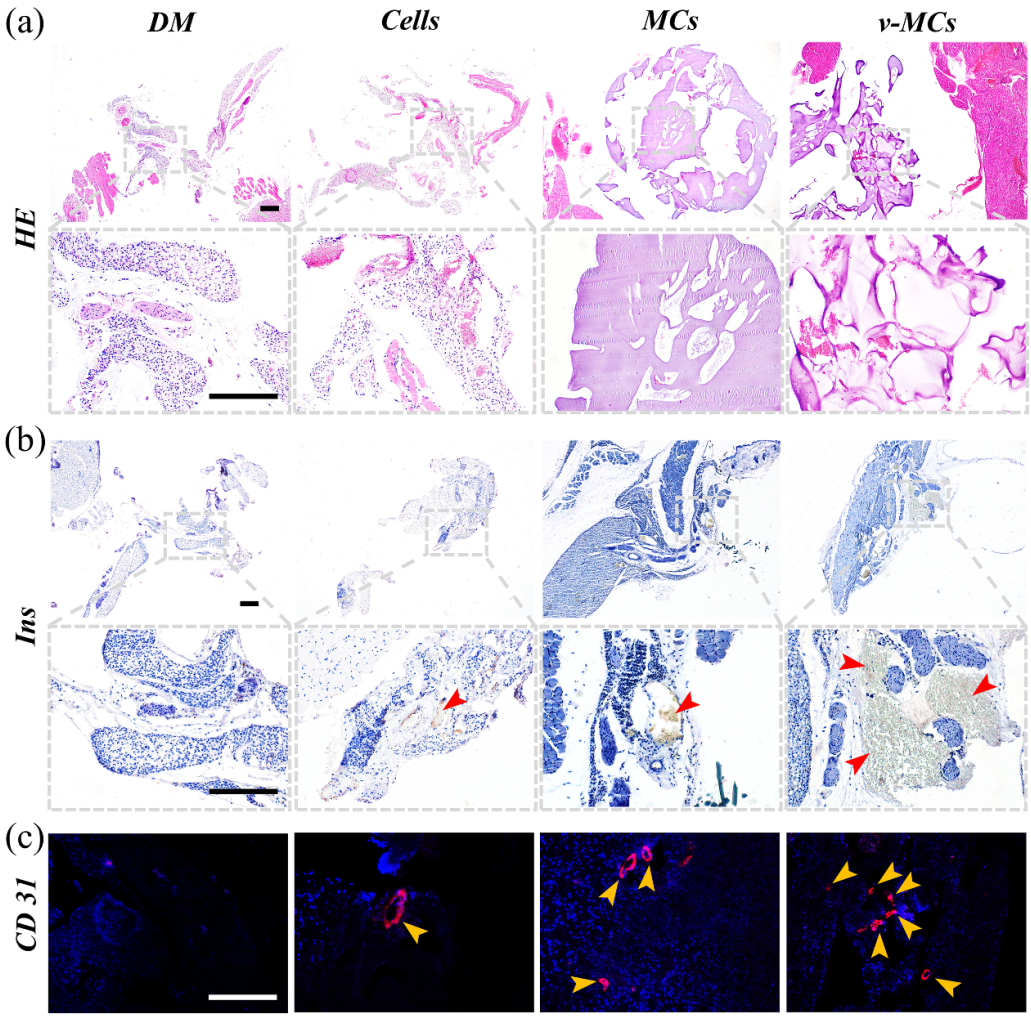

Figure 5. Immunohistochemical and immunofluorescence analysis results. (a) HE staining of the brown adipose tissues and transplanted grafts. (b) Immunohistochemical staining of insulin at the transplantation site. Red arrows indicate insulin-positive areas. (c) Immunofluorescence images of CD31 at the transplantation site. Yellow arrows indicate the microvessels. DM: the diabetes group; Cells: the naked cells group; MCs: the artificial islet microcapsule group; v-MCs: the vascularized artificial islet microcapsule group. Scale bars are 200 μm.

immune-mediated rejection [43]. Benefiting from the insulin secretion, the diabetic mice transplanted with v-MCs (the v-MCs group) demonstrated ameliorated hyperglycemia 3 d after transplantation and maintained normal blood glucose levels for 28 d (figure 4(b)). These cell functions could be attributed to the partial immunoprotective effects of the brown adipose tissues. Although the diabetic mice transplanted with MCs (the MCs group) also showed reduced blood glucose level, it returned to high blood glucose levels in two weeks, probably due to insufficient circulatory networks around the graft site (figure 5(c)). These results suggested the crucial role of vascularization in bolstering engraftment, as well as functionality of the artificial islet microcapsules. In contrast, the control group (the DM group) treated with sham operations demonstrated persistent high blood glucose levels. Besides, the diabetic mice transplanted with bare islet cells (the Cells group) achieved only a temporary decrease in blood glucose level while reversed to previous hyperglycemia two weeks after transplantation. This can be attributed to the lack of a protective layer, where the transplanted cells were damaged by host immune attack, leading to graft failures and severe hyperglycemia similar to sham-operated recipients. These results suggested that transplanted islet models have the promising potential in the diabetic treatment.

Patients with severe diabetes are accompanied by polyphagia and body weight loss. To examine the metabolic states, we also monitored the food intake and body weight of the mice. In Healthy group, the healthy mice showed a steady increase in food intake as well as body weight, when blood glucose levels were maintained within a normal range. It was found that the DM group with continuous high blood glucose levels demonstrated elevated food intake indexes and progressive body weight reduction, suggesting abnormal energy metabolism. Compared with the DM group, the v-MCs and

MCs groups showed limited food intake and reversed body weight equivalent to those of the normal state. Besides, mice in the Cells group took in more food while losing weight, which was consistent with their inability to control blood glucose level. It is noteworthy that the alternation of metabolic states in the v-MCs and MCs groups was correlated with the alleviation of high blood glucose level, which was in accordance with clinical situations (figures 4(c) and (d)). To investigate the glucose tolerance, we employed the IPGTT in various groups at 28th day post transplantation (figure 4(e)). After the glucose bolus administration, the blood glucose levels of the v-MCs group ascended with a relatively smooth trend compared with the rapid rise in the control group. These results revealed the metabolic improvement by transplanting v-MCs and its systemic therapeutic effects on diabetic mice.

Furthermore, histological and molecular analysis were carried out for comfirming the therapeutic function of the islet microcapsule. The HE staining results showed that the v-MCs were transplanted in adipose tissues with vasculatures around. For the Cells group, the HE staining illustrated scarce islet cells with inflammatory infiltrations due to massive islet cell death. Immunochemical staining assays were carried out for detecting insulin (Ins) secreted from pancreatic β cells at the graft site. It was shown that insulin-positive areas of the v-MCs were larger than those in the Cells and MCs groups. In addition, few inflammatory infiltrations were found under histological examinations. By contrast, the microcapsule structure of MCs was confirmed at the graft site yet with less microvessels, which are indicated by immunofluorescence of CD31 (figure 5). Upon the retrival of the graft, contents of the v-MCs were examed via immunofluorescent staining, which showed insulin positive cells encapsulated in the hydrogel shell (figure S8). Furthermore, the safety of transplantation was validated through HE staining for major organs (figure S9). Collectively, the transplantation of v-MCs demonstrated graft survival and security, which laid foundation for practical clinical applications.

4. Conclusion

In conclusion, we have developed microcapsules with microvessels as artificial islet models for glycemic control based on microfluidic electrospray strategy. The design of the microcapsules was inspired by the intrinsic architecture of pancreatic islets possessing a vascularized network. The core-shell MCs allowed entrance of nutrient and oxygen, as well as protection of encapsulated islet cells from host immune cells. Additionally, the v-MCs held the capacity of glucose responsiveness and molecular exchange. Through transplantation of v-MCs, the blood glucose, food intake, and body weight of diabetic mouse models were ameliorated, and the glucose tolerance was promoted given the therapeutic effects of v-MCs. Moreover, *in vivo* engraftment safety of v-MCs was confirmed by histological analyses. These results indicated that the bioinspired artificial islet model with microvessels is valuable for treating diabetes, and future applications in regenerative medicine and tissue engineering can be expected.

5. Future perspectives

In this work, we have successfully developed a bioinspired artificial islet model with vascularized microcapsule structures using a microfluidic electrospray approach, presenting a promising avenue for DM treatment. This model demonstrates potential for achieving long-term glycemic control and enhancing the functionality of transplanted islets. In contrast to conventional methods, our strategy enables the generation of uniform hydrogel microcapsules with a core-shell structure, ensuring efficient encapsulation of islet cells while mimicking the native microenvironment of pancreatic islets. By incorporating microvessels within the microcapsules, we address the challenge of inadequate vascularization, crucial for sustained islet survival and function post-transplantation. The demonstrated enhancements in glucose tolerance, insulin secretion, immune protection, and microcirculation highlight the therapeutic value of the artificial islet model. However, further research is warrented to address challenges such as scalability, long-term stability, and immune compatibility, to realize its full clinical potential. In summary, the development of microcapsules with microvessels represents a notable advancement in islet cell transplantation, offering hope for individuals with diabetes. As we continue to refine our understanding and optimize the design of the biomimetic artificial islet model, it hold promise for transforming diabetes treatment and advancing personalized medicine approaches in the future.

Acknowledgments

This work was supported by National Natural Science Foundation Major International (Regional) Joint Research Program (82320108003), National Natural Science Foundation (82170845, 82000740, 81970717), the Key Research & Development Program (No. BE2022853) and Medical Key Discipline (ZDXK202203) of Jiangsu Province.

Author contributions

L R S and L L conceived the idea and designed the experiment; J B L conducted experiments and data analysis; J B L, L R S and L L wrote the manuscript; Y L F and Z H W assisted in revising the manuscript.

Conflict of interest

The authors declare no competing financial interest.

ORCID iD

Jingbo Li https://orcid.org/0000-0001-8802-4389

References

[1] Magliano D J and Boyko E J 2021 committee IDFDAtes (IDF Diabetes Atlas) Brussels

[2] Hogrebe N J, Ishahak M and Millman J R 2023 Developments in stem cell-derived islet replacement therapy for treating type 1 diabetes *Cell Stem Cell* **30** 530–48

[3] Jain C, Ansarullah, Bilekova S and Lickert H 2022 Targeting pancreatic β cells for diabetes treatment *Nat. Metab.* **4** 1097–108

[4] Rubio-Navarro A *et al* 2023 A beta cell subset with enhanced insulin secretion and glucose metabolism is reduced in type 2 diabetes *Nat. Cell Biol.* **25** 565–78

[5] Shapiro A M J and Verhoeff K 2023 A spectacular year for islet and stem cell transplantation *Nat. Rev. Endocrinol.* **19** 68–69

[6] Chetboun M *et al* 2023 Association between primary graft function and 5-year outcomes of islet allogeneic transplantation in type 1 diabetes: a retrospective, multicentre, observational cohort study in 1210 patients from the collaborative islet transplant registry *Lancet Diabetes Endocrinol.* **11** 391–401

[7] Marfil-Garza B A *et al* 2022 Pancreatic islet transplantation in type 1 diabetes: 20-year experience from a single-centre cohort in Canada *Lancet Diabetes Endocrinol.* **10** 519–32

[8] Li H, Shang Y, Feng Q, Liu Y, Chen J and Dong H 2023 A novel bioartificial pancreas fabricated via islets microencapsulation in anti-adhesive core-shell microgels and macroencapsulation in a hydrogel scaffold prevascularized in vivo *Bioact. Mater.* **27** 362–76

[9] Ernst A U *et al* 2022 A predictive computational platform for optimizing the design of bioartificial pancreas devices *Nat. Commun.* **13** 6031

[10] Wang X *et al* 2021 A nanofibrous encapsulation device for safe delivery of insulin-producing cells to treat type 1 diabetes *Sci. Transl. Med.* **13** eabb4601

[11] Zhang H, Liu Y, Chen G, Wang H, Chen C, Li M, Lu P and Zhao Y 2020 Immunotherapeutic silk inverse opal particles for post-surgical tumor treatment *Sci. Bull.* **65** 380–8

[12] Liu Y, Huang Q, Wang J, Fu F, Ren J and Zhao Y 2017 Microfluidic generation of egg-derived protein microcarriers for 3D cell culture and drug delivery *Sci. Bull.* **62** 1283–90

[13] Zhang B, Cheng Y, Wang H, Ye B, Shang L, Zhao Y and Gu Z 2015 Multifunctional inverse opal particles for drug delivery and monitoring *Nanoscale* **7** 10590–4

[14] Yang L, Liu Y, Sun L, Zhao C, Chen G and Zhao Y 2021 Biomass microcapsules with stem cell encapsulation for bone repair *Nanomicro Lett.* **14** 4

[15] Zhao C, Yu Y, Zhang X, Wu X, Ren J and Zhao Y 2019 Biomimetic intestinal barrier based on microfluidic encapsulated sucralfate microcapsules *Sci. Bull.* **64** 1418–25

[16] Zhao C, Cai L, Nie M, Shang L, Wang Y and Zhao Y 2021 Cheerios effect inspired microbubbles as suspended and adhered oral delivery systems *Adv. Sci.* **8** 2004184

[17] Li Y, Yan D, Fu F, Liu Y, Zhang B, Wang J, Shang L, Gu Z and Zhao Y 2017 Composite core-shell microparticles from microfluidics for synergistic drug delivery *Sci. China Mater.* **60** 543–53

[18] Zhu Y, Sun L, Fu X, Liu J, Liang Z, Tan H, Li W and Zhao Y 2021 Engineering microcapsules to construct vascularized human brain organoids *Chem. Eng. J.* **424** 130427

[19] Yao W, Che J, Zhao C, Zhang X, Zhou H and Bai F 2023 Treatment of Alzheimer's disease by microcapsule regulates neurotransmitter release via microfluidic technology *Eng. Regen.* **4** 183–92

[20] Wang H, Liu Y, Chen Z, Sun L and Zhao Y 2020 Anisotropic structural color particles from colloidal phase separation *Sci. Adv.* **6** eaay1438

[21] Cai L, Zhao C, Chen H, Fan L, Zhao Y, Qian X and Chai R 2022 Suction-cup-inspired adhesive micromotors for drug delivery *Adv. Sci.* **9** 2103384

[22] Heinrich M A, Uboldi I, Kuninty P R, Ankone M J K, van Baarlen J, Zhang Y S, Jain K and Prakash J 2023 Microarchitectural mimicking of stroma-induced vasculature compression in pancreatic tumors using a 3D engineered model *Bioact. Mater.* **22** 18–33

[23] Shang L, Shangguan F, Cheng Y, Lu J, Xie Z, Zhao Y and Gu Z 2013 Microfluidic generation of magnetoresponsive Janus photonic crystal particles *Nanoscale* **5** 9553–7

[24] Liu Y, Sun L, Zhang H, Shang L and Zhao Y 2021 Microfluidics for drug development: from synthesis to evaluation *Chem. Rev.* **121** 7468–529

[25] Shang L, Yu Y, Gao W, Wang Y, Qu L, Zhao Z, Chai R and Zhao Y 2018 Bio-inspired anisotropic wettability surfaces from dynamic Ferrofluid assembled templates *Adv. Funct. Mater.* **28** 1705802

[26] Zhao X, Bian F, Sun L, Cai L, Li L and Zhao Y 2020 Microfluidic generation of nanomaterials for biomedical applications *Small* **16** 1901943

[27] Zhang Y S and Khademhosseini A 2017 Advances in engineering hydrogels *Science* **356** eaaf3627

[28] Yang S, Wang F, Han H, Santos H A, Zhang Y, Zhang H, Wei J and Cai Z 2023 Fabricated technology of biomedical micro-nano hydrogel *Biomed. Technol.* **2** 31–48

[29] Li N, Chen H, Xu D and Zhao Y 2024 Bio-inspired hierarchical particles for bioassays *Biomed. Technol.* **6** 17–25

[30] Chen F, Li X, Yu Y, Li Q, Lin H, Xu L and Shum H C 2023 Phase-separation facilitated one-step fabrication of multiscale heterogeneous two-aqueous-phase gel *Nat. Commun.* **14** 2793

[31] Sun J, Li J, Huan Z, Pandol S J, Liu D, Shang L and Li L 2023 Mesenchymal stem cell-laden composite β cell porous microgel for diabetes treatment *Adv. Funct. Mater.* **33** 2211897

[32] Li J *et al* 2022 Porous microcarriers with pancreatic β cell aggregates loading for diabetic care *Chem. Eng. J.* **436** 135174

[33] Liu X, Yu Y, Liu D, Li J, Sun J, Wei Q, Zhao Y, Pandol S J and Li L 2022 Porous microcapsules encapsulating β cells generated by microfluidic electrospray technology for diabetes treatment *npg Asia Mater.* **14** 39

[34] Zhang H, Chen G, Yu Y, Guo J, Tan Q and Zhao Y 2020 Microfluidic printing of slippery textiles for medical drainage around wounds *Adv. Sci.* **7** 2000789

[35] Wang X, Yu Y, Yang C, Shao C, Shi K, Shang L, Ye F and Zhao Y 2021 Microfluidic 3D printing responsive scaffolds with biomimetic enrichment channels for bone regeneration *Adv. Funct. Mater.* **31** 2105190

[36] Chen G, Yu Y, Fu X, Wang G, Wang Z, Wu X, Ren J and Zhao Y 2022 Microfluidic encapsulated manganese organic frameworks as enzyme mimetics for inflammatory bowel disease treatment *J. Colloid Interface Sci.* **607** 1382–90

[37] Fan L, Zhang X, Wang L, Song Y, Yi K, Wang X, Zhang H, Li L and Zhao Y 2024 Bio-inspired porous microneedles dwelled stem cells for diabetic wound treatment *Adv. Funct. Mater.* 2316742

[38] Zhu Y, Zhang X, Sun L, Wang Y and Zhao Y 2023 Engineering human brain assembloids by microfluidics *Adv. Mater.* **35** 2210083

[39] Yan Y *et al* 2019 Vascularized 3D printed scaffolds for promoting bone regeneration *Biomaterials* **190–191** 97–110

[40] Li G *et al* 2020 Construction of dual-biofunctionalized chitosan/collagen scaffolds for simultaneous neovascularization and nerve regeneration *Research* **2020** 2603048
[41] Cai L, Li N, Zhang Y, Gu H and Zhu Y 2023 Microfluidics-derived microcarrier systems for oral delivery *Biomed. Technol.* **1** 30–38
[42] Zhuge W, Liu H, Wang W and Wang J 2022 Microfluidic bioscaffolds for regenerative engineering *Eng. Regen.* **3** 110–20
[43] Kepple J D, Barra J M, Young M E, Hunter C S and Tse H M 2022 Islet transplantation into brown adipose tissue can delay immune rejection *JCI Insight* **7** e152800